

Rational Design of Materials with Extreme Negative
Compressibility: Selective Soft-Mode Frustration in
 $\text{KMn}[\text{Ag}(\text{CN})_2]_3$

SUPPLEMENTARY INFORMATION

Andrew B. Cairns¹, Amber L. Thompson¹, Matthew G. Tucker²,
Julien Haines³ and Andrew L. Goodwin^{1*}

¹Department of Chemistry, University of Oxford, South Parks Road, Oxford OX1 3QR, U.K.

²ISIS Facility, Rutherford Appleton Laboratory, Harwell Science and Innovation Campus,
Didcot, Oxfordshire OX11 0QX, U.K.

³Institut Charles Gerhardt Montpellier, Équipe PMOF, UMR 5253 CNRS-UM2-ENSCM-UM1,
Université Montpellier II, Sciences et Techniques du Languedoc, Place E. Bataillon cc1504,
34095, Montpellier Cedex 05, France.

*Author to whom correspondence should be addressed;
E-mail andrew.goodwin@chem.ox.ac.uk

1 Synthesis of $\text{KMn}[\text{Ag}(\text{CN})_2]_3$

All reagents were obtained from Aldrich and used as supplied.

1.1 Method 1

$\text{KMn}[\text{Ag}(\text{CN})_2]_3$ was synthesised by a similar method to that reported in Ref. S1. 250.6 mg (1.259 mmol) of $\text{KAg}(\text{CN})_2$ (99%) and 139.9 mg (0.7818 mmol) of $\text{Mn}(\text{NO}_3)_2 \cdot x\text{H}_2\text{O}$ (98%) were each dissolved in 3 ml of H_2O , and these were carefully layered with 2 ml of water and left for 12 h to crystallise, affording 102.1 mg (0.1752 mmol) of $\text{KMn}[\text{Ag}(\text{CN})_2]_3$ (22.41%).

1.2 Method 2

551.8 mg (2.773 mmol) of $\text{KAg}(\text{CN})_2$ (99%) and 269.9 mg (1.929 mmol) of $\text{Mn}(\text{NO}_3)_2 \cdot x\text{H}_2\text{O}$ (98%) were dissolved in a small amount of ice-cold water and placed in separate arms of an H-tube. Cold water was carefully layered on top and left for 14 d in dark conditions, after which time large single crystals had formed (57.4 mg, 0.0985 mmol, 5.11%).

2 Variable Temperature Single Crystal X-Ray Diffraction

Variable temperature single crystal X-Ray diffraction measurements were carried out using a Nonius KappaCCD diffractometer (graphite-monochromated $\text{Mo K}\alpha$ radiation, $\lambda = 0.71073 \text{ \AA}$) fitted with an Oxford Cryosystems cryostream 600 [S2] using a sample prepared as in Method 2. A small crystal ($0.10 \times 0.17 \times 0.18 \text{ mm}$) was mounted on a glass fibre using nail varnish. On cooling from 300 to 100 K, cell parameters were determined every 10 K using $10^\circ \omega$ scans at $\kappa=60^\circ$. Extended data collections were carried out every 50 K using ω -scans as determined by COLLECT [S3] to give a maximum resolution of 0.77 \AA . On heating, cell parameters were measured as above, but only at intervals of 25 K. We found no evidence for any hysteretic behaviour.

Cell parameters were determined and data reduction carried out using DENZO/SCALEPACK [S4]. Structure solution was carried out for the 100 K data using SIR92 [S5] within CRYSTALS [S6]. In all cases it was possible to solve the structure completely in this way; however in practice we used the final coordinates obtained from the 100 K data set as a starting model for subsequent structure solutions. In all cases an extinction parameter [S7] was refined, and a four-parameter Chebychev polynomial weighting scheme [S8–S10] used to optimise weights. Selected crystallographic data are presented in Table S1. Lattice parameters measured in the variable-temperature runs are listed in Table S2, and plotted in Fig. S1. The relatively narrow- ω collection strategy resulted in some difficulties in standard error determination within the DENZO/SCALEPACK routines. A number of the standard error values calculated in this way were judged to be too small by up to two orders of magnitude. The subset of temperature values for which reliable error values could be obtained were used to estimate an “average” standard error, which has been substituted for the too-small values obtained at the remaining temperatures. While the strategy can clearly be improved, we note that our aim here is to obtain estimates of the coefficients of thermal expansion of $\text{KMn}[\text{Ag}(\text{CN})_2]_3$, and these values are largely unaffected by the uncertainties in standard error.

3 Variable Pressure Powder Neutron Diffraction

For the variable pressure measurements, a sample of approximately 100 mg prepared according to method 1 was ground to a fine powder and loaded into an encapsulated titanium zirconium (TiZr) gasket [S11]. A deuterated methanol-ethanol mixture, in the ratio of 4 to 1, was added as a pressure transmitting medium and a small lead sphere was placed in the centre of the sample as a pressure marker. This assembly was then sealed between two boron nitride (BN) anvils within a VX4 Paris-Edinburgh (P-E) press [S12] by applying an initial load of 70 bar. The gasket TiZr was alloyed in the correct proportions so as to have an average coherent neutron scattering length of zero and so does not produce any background Bragg reflection. The BN anvils are often referred to as “self collimating” since boron is a good neutron absorber and so they also do not produce background Bragg reflections. Data were collected as a function of neutron time-of-flight as 0.5 h runs using the WISH diffractometer at the ISIS facility.

The resulting normalised powder diffraction patterns were analysed by using the GSAS Rietveld refinement package using a multiphase refinement including the sample and the Pb pressure marker [S13]. This was the first time this press was mounted on the WISH instrument and as such the setup was not fully optimised. This meant there was a small background of parasitic Bragg peaks from the experimental assembly and these peaks were not included in the Rietveld fit [Fig. S3]. Sample pressures were obtained by fitting the measured Pb lattice parameter to the known equation of state for Pb ($dP \simeq 0.15\text{-}0.2$ GPa). The lattice parameter values obtained are listed in Table S3, and the corresponding GSAS fits are shown in Fig. S2.

Given the small sample quantities involved in P-E measurements, and the relatively short data collection time, the data were not of sufficient quality to allow for unambiguous refinement of atomic positions. Consequently the atomic coordinates determined using single-crystal X-ray diffraction under ambient conditions were used and fixed in all Rietveld refinements of these neutron data. We hope to be able to perform a more in-depth structural analysis in the near future.

We note that there is a relatively large increase in peak width between 1.20 and 1.52 GPa, with this broadening increasing further at high pressures. Some peak broadening on application of hydrostatic pressure is to be expected, but it is not altogether clear to us why the rate of broadening changes so abruptly. Our initial hypothesis was that this effect might be due to a small monoclinic distortion of the cell; however refinements of the related $C2$ cell against the 1.52 GPa data converged to within error to the original $P312$ metric. The relatively large compressibilities (both positive and negative) of $\text{KMn}[\text{Ag}(\text{CN})_2]_3$ mean that any pressure inhomogeneities or anisotropic strain terms will result in more noticeable broadening than would otherwise be the case, and we are left to assume that this is the probable origin of the effect. In our previous work with $\text{Ag}_3[\text{Co}(\text{CN})_6]$ we also observed very unusual peak broadening effects with temperature [S14], and it is relevant to note that we also observed there a discontinuous variation in the refined strain broadening term as a function of temperature.

Table S1. Crystallographic details determined by Single Crystal X-ray Diffraction for $\text{KMn}[\text{Ag}(\text{CN})_2]_3$.

empirical formula	$\text{KMnAg}_3\text{C}_6\text{N}_6$				
formula weight	573.74				
crystal colour	colourless				
crystal size (mm)	$0.18 \times 0.17 \times 0.10$				
crystal system	trigonal				
space group	$P\bar{3}12$ (No. 149)				
Z	1				
radiation	Mo K_α				
temperature (K)	100	150	200	250	300
a (Å)	6.8214(2)	6.8431(2)	6.8660(2)	6.8904(2)	6.9154(2)
c (Å)	8.2353(4)	8.2137(4)	8.1895(4)	8.1649(4)	8.1399(4)
V (Å ³)	331.86(2)	333.10(2)	334.35(2)	335.71(2)	337.12(2)
μ (mm ⁻¹)	5.586	5.565	5.544	5.522	5.499
reflns ($I > 3\sigma(I)$)	390	515	511	513	512
R (F_o)	0.0178	0.0237	0.0242	0.0287	0.0280
R_w (F_o)	0.0420	0.0598	0.0599	0.0694	0.0654
GOF	0.9328	0.9461	0.8782	0.9169	0.8527

Table S2. Variable temperature lattice parameter data as determined using single crystal X-Ray diffraction.

T (K)	a (Å)	c (Å)	V (Å ³)
300	6.916(16)	8.142(21)	334.96(21)
300	6.920(16)	8.146(19)	335.58(20)
290	6.913(11)	8.138(23)	334.53(18)
280	6.906(16)	8.151(21)	334.37(21)
275	6.906(15)	8.145(18)	334.13(18)
270	6.901(16)	8.155(21)	334.12(21)
260	6.895(16)	8.159(21)	333.65(21)
250	6.889(26)	8.16(4)	333.2(3)
250	6.893(14)	8.155(17)	333.33(18)
240	6.892(15)	8.167(18)	333.69(19)
230	6.878(16)	8.177(21)	332.79(21)
225	6.877(16)	8.178(21)	332.72(21)
220	6.877(16)	8.184(19)	332.93(20)
210	6.873(15)	8.203(19)	333.34(19)
200	6.871(22)	8.21(3)	333.34(29)
200	6.866(16)	8.192(21)	332.20(21)
190	6.862(16)	8.193(21)	331.83(21)
180	6.865(15)	8.212(19)	332.96(19)
175	6.854(16)	8.204(21)	331.55(21)
170	6.852(16)	8.202(21)	331.23(21)
160	6.857(16)	8.226(21)	332.68(20)
150	6.849(16)	8.215(21)	331.45(21)
150	6.854(16)	8.216(21)	332.06(21)
140	6.841(15)	8.214(21)	330.67(20)
130	6.841(15)	8.217(21)	330.79(20)
125	6.822(14)	8.211(19)	328.78(18)
120	6.841(15)	8.218(21)	330.81(20)
110	6.837(15)	8.218(21)	330.46(20)
100	6.840(15)	8.230(21)	331.22(20)

Table S3. Variable pressure lattice parameter data as determined using neutron powder diffraction.

p (GPa)	a (Å)	c (Å)	V (Å ³)
0.22(12)	6.82042(15)	8.1961(5)	330.186(17)
0.50(15)	6.73777(19)	8.2387(6)	323.91(2)
0.86(12)	6.64413(19)	8.2842(6)	316.706 (21)
1.20(17)	6.56392(3)	8.3215(9)	310.50(3)
1.52(17)	6.4973(6)	8.3543(22)	305.42(8)
1.78(15)	6.4543(8)	8.3722(27)	302.04(9)
1.98(15)	6.427(9)	8.377(3)	299.66(11)
1.95(18)	6.4227(10)	8.382(4)	299.43(12)
2.15(15)	6.3888(9)	8.387(3)	296.47(11)

Figure S1. Thermal lattice parameter variation for $\text{KMn}[\text{Ag}(\text{CN})_2]_3$ as determined by single crystal X-Ray diffraction.

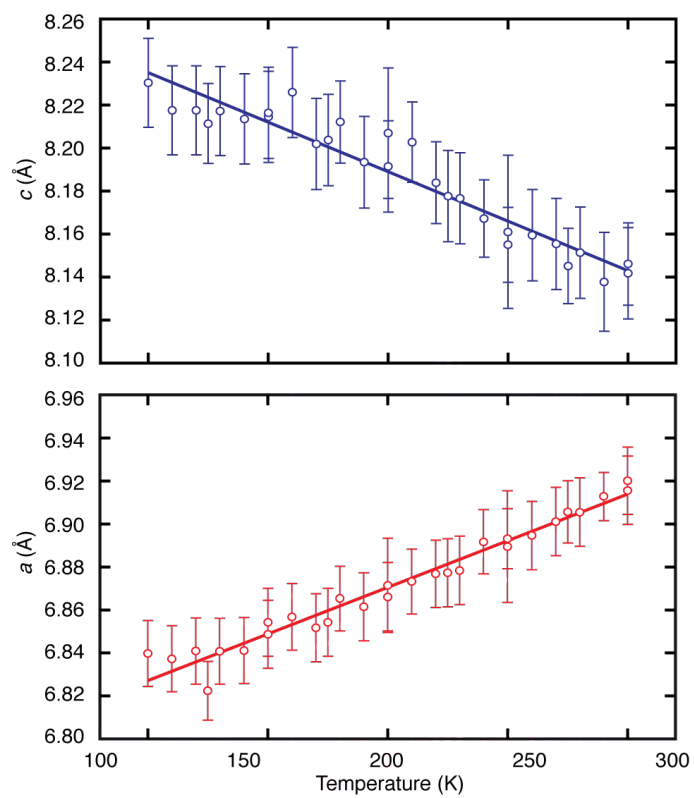


Figure S2. GSAS fits (red) to neutron powder diffraction data (black), with difference curves (data–fit) shown in blue. Successive data sets are shifted upwards in the vertical axis by units of one; difference curves are shifted downwards along the same axis by 0.1 units.

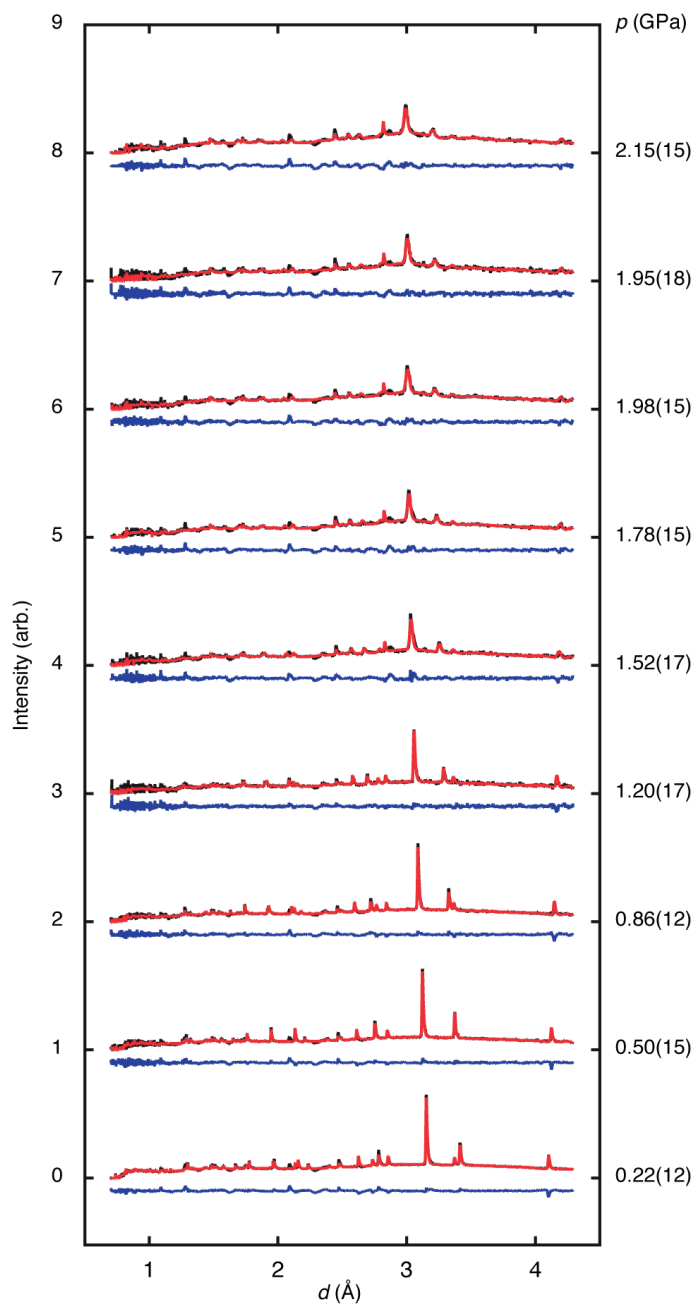
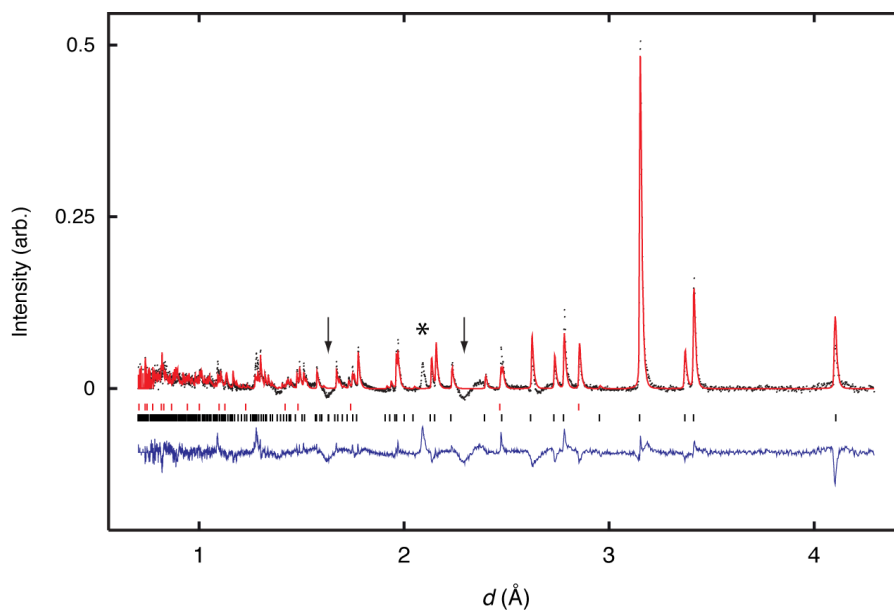


Figure S3. Background-subtracted GSAS fit (red) to neutron powder diffraction data (black) collected at 0.22 GPa, with difference curve (data–fit) shown in blue. Tick marks correspond to $\text{KMn}[\text{Ag}(\text{CN})_2]_3$ (black) and Pb (red). The as-yet uncharacterised background features include some signal attenuation (arrows) and also at least one spurious Bragg peak (asterisk).



References and Notes

- [S1] Geiser, U.; Schlueter, J. A. *Acta Crystallogr., Sect. C* **2003**, *59*, i21.
- [S2] Cosier, J.; Glazer, A. M. *J. Appl. Crystallogr.* **1986**, *19*, 105.
- [S3] Nonius, B. V. *Collect*; Delft, The Netherlands, 2001.
- [S4] Otwinowski, Z.; Minor, W. *Meth. Enz.: Macromol. Crystallogr. A* **1997**, *276*, 307.
- [S5] Altomare, A.; Cascarano, G.; Giacovazzo, C.; Guagliardi, A.; Burla, M. C.; Polidori, G.; Camalli M. *J. Appl. Crystallogr.* **1994**, *27*, 435.
- [S6] Betteridge, P. W.; Carruthers, J. R.; Cooper, R. I.; Prout, K.; Watkin, D. J. *J. Appl. Crystallogr.* **2003**, *36*, 1487.
- [S7] Larsen, A. C. in *Crystallographic Computing*, Eds. Ahmed, F. R.; Hall, S. R.; Huber, C. P.; Munksgaard, Copenhagen, 1970, pp. 291-294.
- [S8] Prince, E. *Mathematical Techniques in Crystallography and Materials Science*; Springer-Verlag, New York, 1982.
- [S9] Carruthers, J. R.; Watkin, D. J. *Acta Cryst.* **1979**, *A35*, 698-699.
- [S10] Watkin, D. J. *Acta. Cryst.* **1994**, *A50*, 411-437.
- [S11] Marshall, W. G.; Francis, D. J. *J. Appl. Crystallogr.* **2002**, *35*, 122.
- [S12] Klotz, S.; Hamel, G.; Frelat, J. *High Press. Res. Int. J.* **24**, 219 (2004).
- [S13] von Dreele, R.; Larson, A. C. *General Structure Analysis System (GSAS)*. Los Alamos National Laboratory Report LAUR 86-748, 1986.
- [S14] Goodwin, A. L.; Calleja, M.; Conterio, M. J.; Dove, M. T.; Evans, J. S. O.; Keen, D. A.; Peters, L.; Tucker, M. G. *Science* **319**, 794 (2008).